Dish Optical-Structural Interactions: Characterization and Modeling

Charles E. Andraka[1], Nolan Finch[2], Julius Yellowhair[2], Matt Francis[3], Kirby Hunt[3], Tom Kulaga[4]

[1] Sandia National Laboratories, PO 5800 Albuquerque NM USA 87185-1127, (505)844-8573,: ceandra@sandia.gov

[2] Sandia National Laboratories, PO 5800 Albuquerque NM USA 87185-1127

[3] Stirling Energy Systems,4800 Scottsdale Road, Suite 5500, Scottsdale AZ 82521

[4] Solution Stream Engineering, Phoenix AZ

Abstract

Sandia National Laboratories has developed the AIMFAST system, based on fringe reflection methods, to characterize and perform alignments on dish concentrators. The system has been successfully applied to the Stirling Energy Systems (SES) dish Stirling systems, with a noted improvement in performance and flux patterns. The system is used at the service position (below horizon) to facilitate 2f alignments. The alignment is corrected to 40 degrees elevation through a Finite Element Analysis (FEA) of the dish structure, accounting for gravity-induced structural deflection differences between the alignment position and "golden" operation condition.

The accurate alignment of the dish system relies upon an accurate FEA, particularly for deflections that manifest as free-body rotation of the facets. Since the actual data collection equipment for AIMFAST is compact, consisting of a camera and large screen LCD television, it is feasible to position the system at various elevation angles and characterize the dish. In the current work, we characterize the dish at the service position, and every 10 degrees elevation from horizon to 60 degrees. We then compare the measured facet rotations to the FEA model. In addition, we calculate the impact of these rotations on the flux pattern near the engine heater head, and compare the flux pattern to that measured by fluxmapper tools.

Keywords: Dish, Stirling, Alignment, Gravity, Optics, Distortion

1. Introduction

Modern dish systems often include a structural steel or aluminum back assembly supporting individual facets making up or approximating a parabola of revolution. The design of the structure must conserve material to keep costs minimal, but also preserve facet alignment though a varying gravity vector. It is important to understand the structural motions and their impact on the flux profile at the receiver absorber, in order to optimize the design for system performance and life. Facet motions cause systematic mirror slope deviations (rotations), which can lead to high peak fluxes on the receiver [1], and can shorten engine life and reduce performance. The design process typically includes FEA analysis of the support structure, and treats the facet modules as rigid bodies on pivoting mounting points.

If one understands the facet motion, an ideal elevation angle for a design alignment can be determined. This angle will depend on the net influences of the gravity vector on flux profile. The ideal alignment elevation angle will likely be within the range of sun tracking, and not at an elevation convenient for implementing alignment. Typically alignment is physically implemented at 0 degrees, 90 degrees, or "service" position (below horizon). An accurate understanding of the structural deflections from this position to the ideal tracking elevation will allow a "deviated" alignment at the alignment position which results in a near-perfect alignment in tracking.

Due to computational limits, no FEA model is perfect. Often simplifications include beam analysis with simplified joint geometries. In addition, material thicknesses and section sizes vary within a specified range. It is important that net facet rotations be accurately determined. Facet rotations of 0.25 mrad RMS have been shown to lead to high peak fluxes on the receiver [1]. The AIMFAST tool accurately determines the facet rotations, usually for the purpose of alignment [2]. The tool has been modified to allow positioning near twice the focal length (2f location) at various dish elevations. The resulting relative facet rotations can then be compared to the FEA models.

2. Implementation

The AIMFAST system consists of a 70-inch class monitor (1.78m diagonal measurement) with a camera viewing the dish facets from near the 2f location (Figure 1). The system used in this paper does not include the color panels surrounding the monitor. These panels are used in automated alignments to help locate a poorly preset facet. The AIMFAST system uses photogrammetry to determine the system orientation to the dish coordinate system, and this is "trued up" using laser distance measurements to a few key locations on the dish. The camera images the reflection of the TV screen in the mirrors as multiple fringe patterns are displayed on the screen. Using fringe reflection methods (Deflectometry) [2, 3], the return location on the screen of each camera pixel can be determined, and thus the surface normal vectors of the facets can be determined. Typically, 20,000 points are located on each facet. Ulmer [4] and Heimsath [5] pioneered the implementation of fringe reflection methods for characterization of CSP systems, and Andraka [2] has extended these approaches to computer-controlled alignment processes. The system can collect the data in about 2 seconds, and reduce the data for all 40 facets in another 3-4 seconds. This system was mounted to a forklift stand with tilt capabilities to characterize the dish. The short data collection period minimized concerns over system temporal stability.

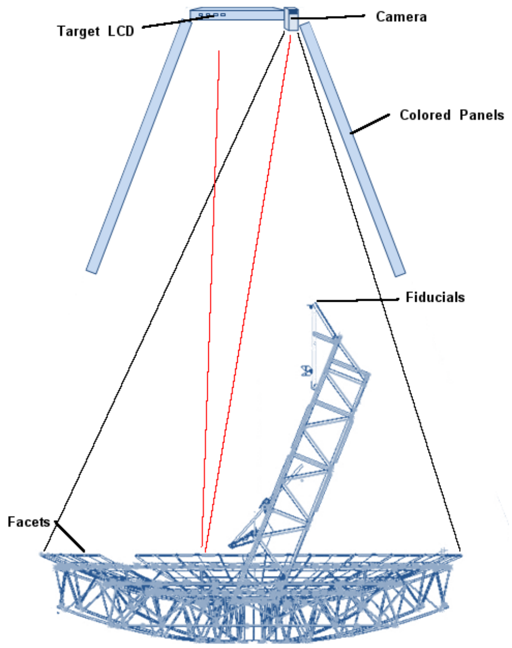

Figure 1. AIMFAST system layout. The truck-mounted system used in this paper does not include the colored panels.

AIMFAST provides the rotation of each facet compared to a design alignment strategy, by averaging the measured surface normal error compared to design at each point on the facet. In addition, AIMFAST can provide characterization of each facet in situ, based on about 20,000 measured points on each facet. AIMFAST also provides a field of surface normal vectors, which can be used in a ray trace or optical model, such as Sandia's CIRCE2 [6], to predict flux patterns on a flat or shaped receiver surface.

In this series of tests, after aligning the dish at -20 degrees elevation, we measured the facet rotations at 10 degree increments from -20 degrees to 60 degrees elevation (Figure 2). The maximum measured elevation was limited by the reach of the forklift used to position the AIMFAST data collection system. Given the measured facet rotations relative to the alignment strategy at two different dish elevations, we difference the cases to determine the relative rotation of the facets due to a changing gravity vector.

A Finite Element Analysis (FEA) model of the dish structure was built in HyperWorks by Altair. The model represented the entire dish structure, and so was limited to shell and beam elements for computational efficiency. The mirror facets are mounted to the support frame with three mounting posts, each with a swivel joint to the mirror backing. The mirror shape was not modeled in the FEA model. Each facet was modeled with a massless, 0-stiffness RB3 element with a lumped mass at the facet center of gravity. This method allows the mirror mass to be properly distributed to the mounting points, but does not account for loads that may arise due to the stiffness of the facet, nor shape changes of the facet itself. The facet elements also contained points of interest, such as the visible splits between glass segments on the front surface, so that rotations can be evaluated at the visible physical locations. The calculated rotations and translations were reported at each key point on the facet element. The dish structure is supported in the FEA model, as in real life, at the elevation pivot axel and the elevation drive trunion. The entire model is a linear, elastic model, without nonlinear features such as friction in sliding joints.

Figure 2. AIMFAST elevation-dependent measuremetn of SES dish. The LCD TV screen and camera are located on a forklift near the 2f point.

The AIMFAST dish coordinate system z axis is tied to a line from the theoretical center of the facet system to the center of the engine aperture, as determined by the fiducials mounted at the end of the boom. Thus, the alignment is made to the engine center rather than perpendicular to the “plane” of the facets. Therefore, if there is boom bending with gravity, there will be an apparent mean rotation applied to all of the facets. Similarly, if the boom section between the elevation drive and the facet support structure bends, a mean rotation can be induced in the FEA model. For the purposes of the comparisons in this paper, we subtract out the mean facet rotation, both on the measured data and on the FEA data. While this approach does not perfectly align the coordinate systems, it provides a simple, reasonable approach for direct comparison. A more accurate, but more difficult approach would be to determine the rotation of a coordinate system aligned with the optical axis of the facets. However, since the origin of this coordinate system is a hypothetical point in space, and the facets move relative to each other, it would be difficult to accurately monitor the orientation of the coordinate system in a consistent manner between the FEA and AIMFAST tools.

A flat-target fluxmapper system was used to confirm the character of the flux profile at each elevation angle. This fluxmap is qualitatively and semi-quantitatively compared to CIRCE2 optical modeling of the AIMFAST measurements of the complete dish system. In order to represent field conditions, the service-position-measured facet normals were rotated by the FEA-determined amounts to each tracking position, and a CIRCE2 prediction of the fluxmap profile generated. In addition, at each AIMFAST-measured elevation, a CIRCE2 model was directly generated from the collected AIMFAST surface normals. These CIRCE2 results could be compared to determine the accuracy of the FEA model, and the impact of FEA errors on the flux profiles. Finally, A CIRCE2 model was used to predict the flux profiles on a non-flat receiver cavity, for both the FEA-rotated alignment data and the measured data at 40 degrees elevation.

3. Results

The relative facet rotations were determined by FEA and by AIMFAST for a change in dish position from the service position at -20 degrees elevation to the design "perfect' alignment elevation of 40 degrees. This selection of data represents the error that would be introduced in the alignment were the rotation predictions not taken into account. Figure 3 shows a comparison of the facet rotations as predicted by FEA (red), measured by AIMFAST (green), and the difference between the two (cyan). The outer facets exhibit an alternating pattern of deflection, attributed to the alternating support (along radials, between radials) of the facet posts on adjacent facets. Note that the errors indicated by the cyan vectors indicate that the FEA over-predicts radial "blooming" of the outer facets fairly consistently. The inner facets show a smaller and less systematic difference between prediction and measurement.

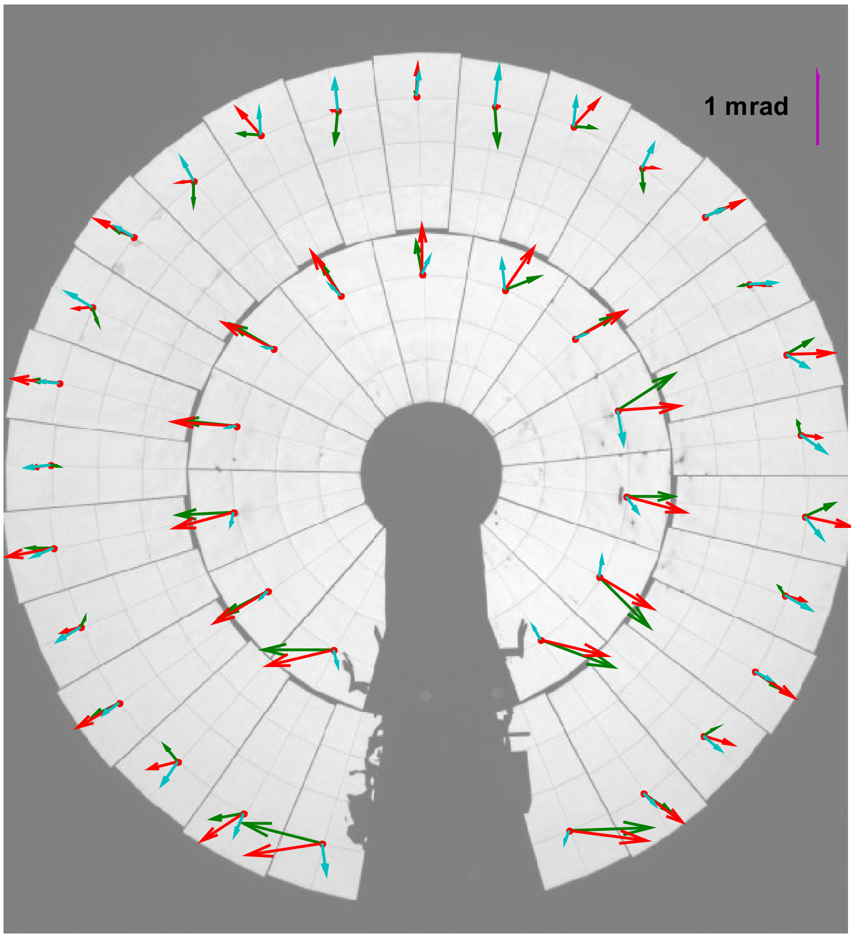

Figure 3. Facet rotation comparison, FEA to AIMFAST measurement, for a dish rotation from -20 degrees to 60 degrees elevation. The red vectors are FEA, green are AIMFAST measurements, and cyan are the difference between the two. All vectors have the same scaling.

We next compared measurements and predictions to rotate the dish from 20 degrees to 60 degrees elevation. This rotation avoids gravity vector reversals on the facets, so that if there is any free play in the mounts, nonlinear effects are avoided. Figure 4 shows the comparison between the FEA predictions and the AIMFAST measurements. Overall, the comparison (cyan) appears better than the prior case, though the rotation angle of the gravity vector is less.

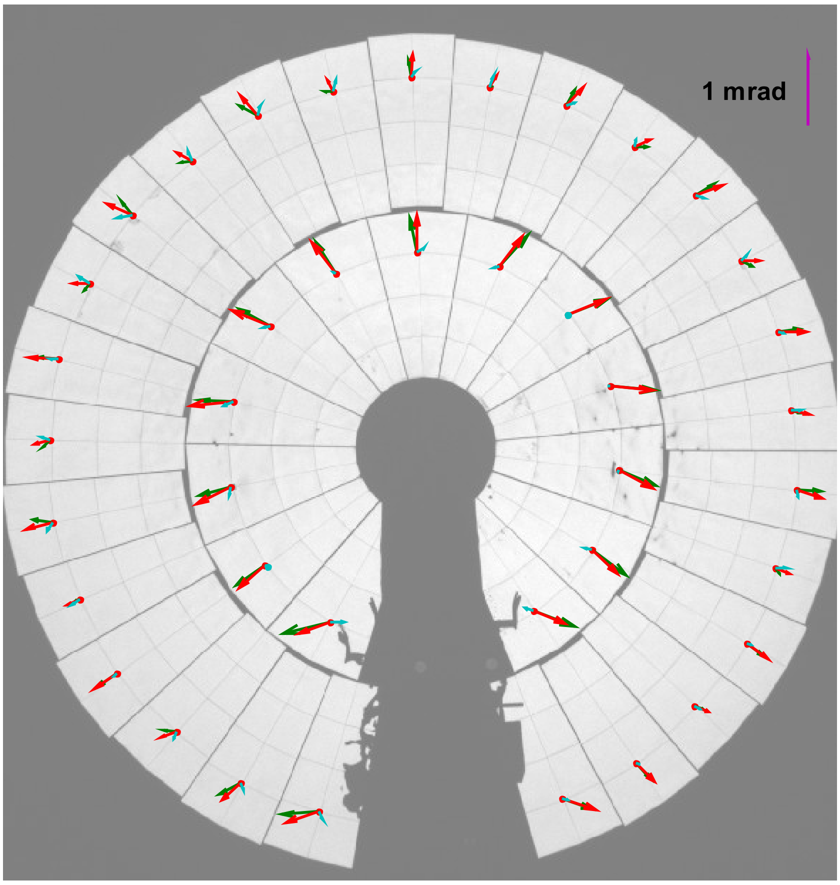

Figure 4. Facet rotation comparison, FEA to AIMFAST measurement, for a dish rotation from +20 degrees to +60 degrees elevation.

The measured facet normals can be modeled in CIRCE2 to predict the incident flux pattern on a flat plate or receiver cavity. We predict on a flat plate at 6.909m (272") from the dish vertex, which is near the center of the engine heater head tube bundle, and compare to flat plate fluxmapper results. In all cases, the tracking, or sun position relative to the dish, is adjusted such that the center "valley" in the flux is centered on the analytical target. The first set of predictions is based on the post-alignment condition at the service (alignment) position. These measured normals are rotated by the FEA predictions to the various tracking elevations. These are shown in the left column of Figure 5. In the second case, the measured surface normals at various dish elevations are modeled in CIRCE2, and again projected onto a flat plate target. These results are shown in the right hand column of Figure 5. As the elevation increases, observe that the "V-notch" at the top of the flux image, caused by the pedestal gap in the dish, closes and eventually gives way to a peak flux in this area. Also observe that as elevation increases, the measured-in-place case has a smaller center "valley" in the flux, and the FEA-rotated cases have a ring of flux with greater magnitude than the measured cases.

In the next case, the flux is measured on a flat target using standard Beam Characterization techniques, in which a camera with filters is used to image a Lambertian plate at the desired location. The beam is centered on the plate, and the image is scaled such that the total energy on the plate equals the CIRCE2 prediction. The measurement was made at 45 degrees elevation. Figure 6 shows a comparison between the FEA-rotated CIRCE2 prediction at 45 degrees and the fluxmap. No direct AIMFAST measurement was available at 45 degrees, and fluxmapping was only available at 45 degrees. The color scales match the prior figure.

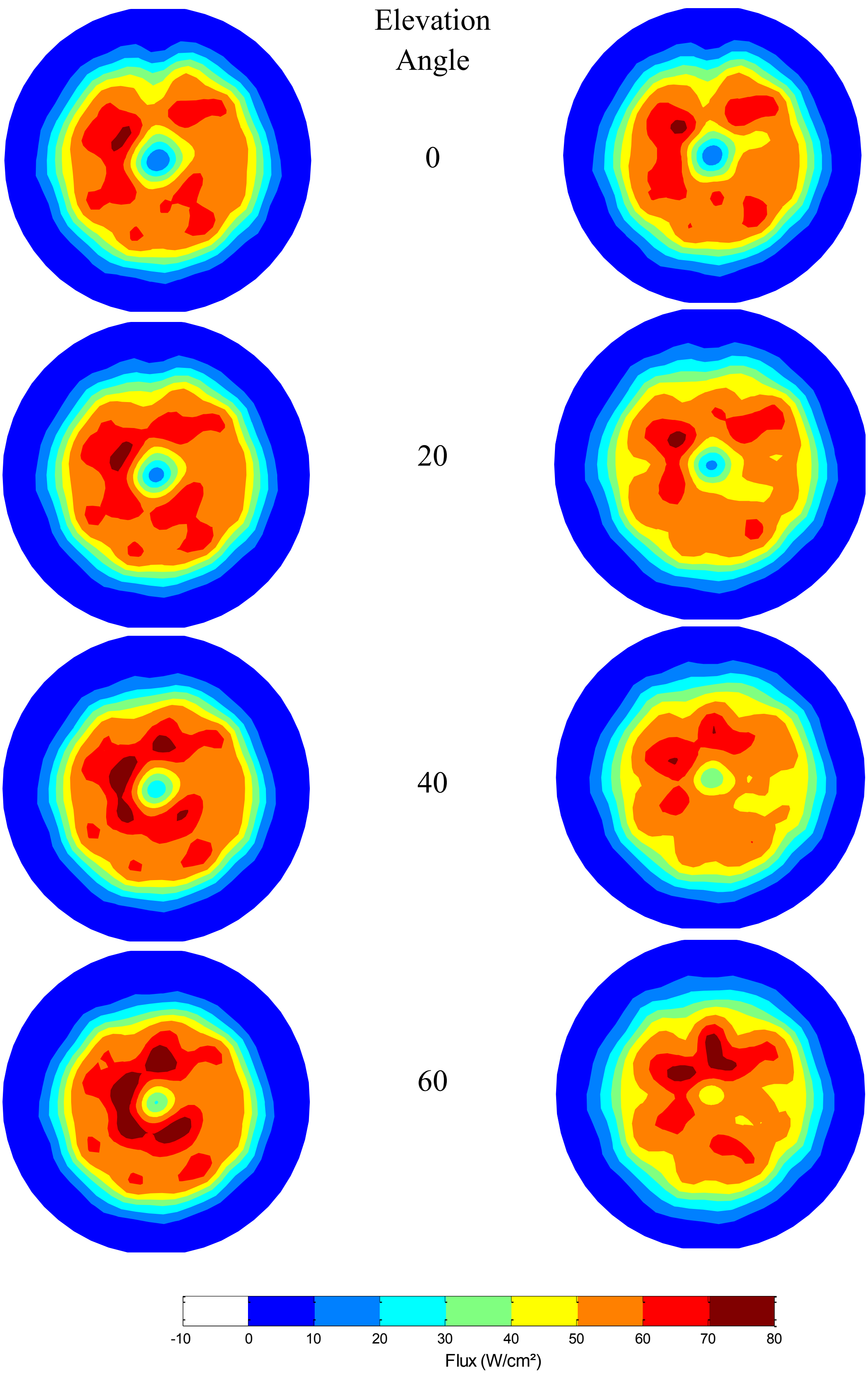

Figure 5. CIRCE2 predictions of flux on flat plates. Left is rotated from service, right is measured in place. The plate is 0.6m in diameter.

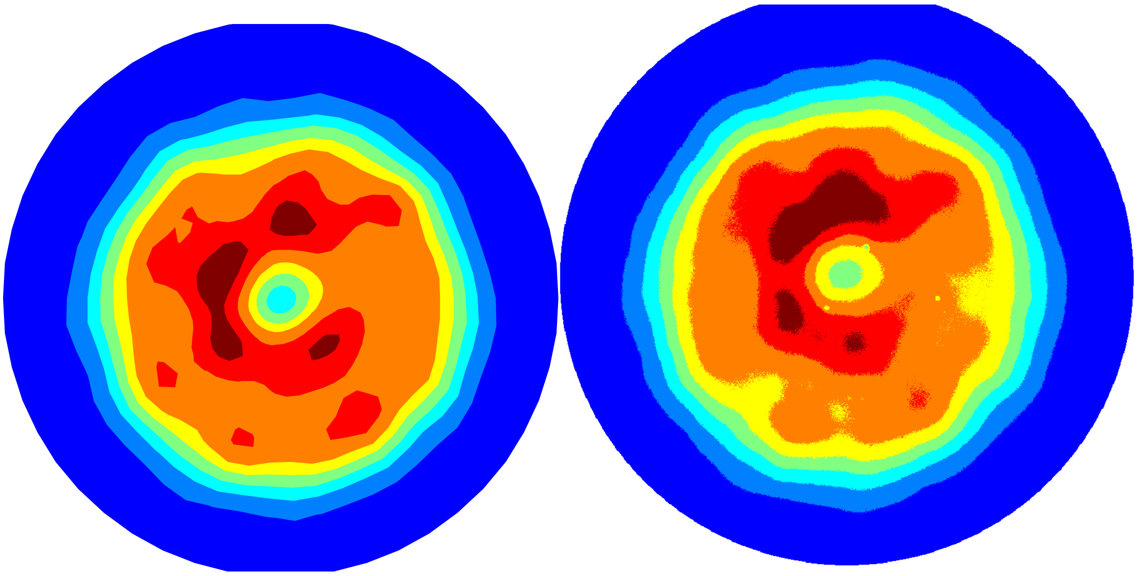

Figure 6. Comparison of CIRCE2 prediction using FEA to rotate from -20 degrees to 45 degrees (left), and fluxmap measured at 45 degrees (right).

4. Discussion

In Figure 3, the FEA appears to over-predict the outer facet rotations in the radial direction ("blooming"), though this is not generally the case on the inner facets. It is likely that a part of the model affecting only the outer facets does not match the hardware implementation. The outer posts of the outer facet are supported by a tangential steel member, which is symmetrically supported under each facet. The inner ends are supported in alternating ways, one on the radial and the next centered on a tangential member. Thus, it is likely the issue is that the FEA model under-predicts the stiffness of the outer tangential member, or the rotational stiffness of the supporting joints. The errors in facet rotation are radial, and on the order of 0.5 mrad. This amounts to a displacement error at the mounting points of about 0.6mm.

Figure 4, while covering a smaller angular displacement, avoids a reversal in gravity load, eliminating potential hysteresis or other nonlinear impacts. In this case, the agreement between the FEA and the actual dish appears to be far better. Thus, perhaps play in a joint in the facet mounting system is impacting the measurements, and offsetting some actual blooming of the dish.

While prior work [1] has shown a random alignment error should be limited to 0.25 mrad, the alignment error resulting from this discrepancy is nearly purely radial. In addition, as the dish rotates upward, the facet tip back, causing an inward motion of the flux pattern on a plane behind the focal plane. However, the error noted is that the facets rotate *less* than predicted, and therefore less overlap between outer and inner facet images should be observed. This is borne out in the flux profiles of Figure 5. Therefore, the observed error should not increase peak fluxes detrimentally.

In Figure 5, we do observe a ring of higher flux in the FEA-rotated images, matching our observations above. We also note that the AIMFAST-measured data (RHS) shows less of a "valley" in the middle of the flux profile, while the rotations of inner facets in Figure 3 would not explain this issue. Upon review of the facet characterization by AIMFAST in each location, we find that the average focal length of the inner facets is 6.728m when measured at the service position, and at 60 degrees elevation the average focal length is 6.683, a 45mm change in focal length. The shorter focal length results in a larger image (behind the focal plane), and thus closes the center valley in the flux. A similar change in focal length is seen on the outer facets. It is possible that this facet shape change impacts the facet rotations, since the facet is modeled as an element with no stiffness. The facet may be contributing to the overall system stiffness.

In Figure 6 we see a reasonable qualitative match between the fluxmap and the prediction, using FEA rotations form the -20 degree position. Unfortunately, the data collection during fluxmapping was not coordinated with the alignment team, and so data at the same elevation is not available. The fluxmap does show a smaller center valley, which agrees with the AIMFAST measurements at similar angles, confirming the apparent change in facet focal lengths.

5. Conclusions

The rotations of the facets due to the changing gravity vectors is significant, over 1 mrad typical, and therefore must be accounted for when aligning at a position other than the "golden" angle. While we implemented an FEA model to determine the rotations and implement an alignment, it is apparent in these measurements that there are radial rotation differences in the FEA compared to the dish as implemented. The differences, systematic in nature, do not negatively impact the flux pattern on the receiver surface.

In future work, the following is recommended:

1. Determine the source of the FEA discrepancy, and implement modified FEA model results in the alignment code.
2. Consider empirically determining "standard" facet rotations rather than relying on design FEA. However, this should be repeated on a number of dishes, and an average taken.
3. Include facet shape in the FEA model, so that any feedback from shape change into the structural deflections is taken into account.

Acknowledgements

This manuscript has been authored by Sandia Corporation under Contract No. DE-AC04-94AL85000 with the U.S. Department of Energy. The United States Government retains and the publisher, by accepting the article for publication, acknowledges that the United States Government retains a non-exclusive, paid-up, irrevocable, world-wide license to publish or reproduce the published form of this manuscript, or allow others to do so, for United States Government purposes.

The authors would like to thank Stirling Energy Systems for access to their systems during the development of AIMFAST, and access to data for this paper. The cooperation with SES has made significant advances in dish-Engine technology possible.

References

[1] Andraka, C.E., Yellowhair, J, Iverson, B.D., (2009). "A Parametric Study of the Impact of Various Error Contributions on the Flux Distribution of a Solar Dish Concentrator", Proceedings of the ASME 2010 4th International Conference on Energy Sustainability, Paper ES2010-90242, ASME, Phoenix AZ USA May 17-22.

[2] Andraka, C.E., Yellowhair, J, Finch, N., Carlson, J., Francis, M., Hunt, K., Raffa, C., Kulaga, T., (2011). "AIMFAST: Initial Dish System Alignments Results Using Fringe Reflection Methods", Proceedings of the ASME 2011 5th International Conference on Energy Sustainability, Paper ES2011-54453, ASME, Washington DC USA August 7-10.

[3] Bothe, T., Li, W., von Kopylow, C., Jüptner, W., (2004),"High Resolution 3D Shape Measurement on Specular Surfaces by Fringe Reflection", Optical Metrology in Production Engineering, Proceedings of SPIE Vol. 5457, Bellingham, WA. USA

[4] Ulmer, S., Marz, T., Prahl, C, Reinalter, W., Belhomme, B. (2011), "Automated High Resolution Measurement of Heliostat Slope Errors", *Solar Energy*, Vol 85, p681-687.

[5] Heimsath, A., Platzer, W., Bothe, T., Wansong, L. (2008), "Characterization of Optical Components for Linear Fresnel Collectors by Fringe Reflection Method", *Proceedings of Solar Paces Conference*, Las Vegas, NV USA.

[6] Romero V. J. (1991), "CIRCE2/DEKGEN2: A Software Package for Facilitated Optical Analysis of 3-D Distributed Solar Energy Concentrators – Theory and User Manual," SAND91-2238, Sandia National Laboratories, Albuquerque, NM